Submitted to J. Phys. Chem. Lett., 6/23/2021, revised 7/28/2021

Dynamics of Initial Hydrogen Spillover from Single Atom Pt Active Site to the Cu(111) Host Surface: The Impact of Substrate Electron-Hole Pairs

Kaixuan Gu,[1] Fenfei Wei,[1] Yuhui Cai,[1] Sen Lin,[1,*] and Hua Guo,[2,*]

[1]*State Key Laboratory of Photocatalysis on Energy and Environment, College of Chemistry, Fuzhou University, Fuzhou 350002, China*

[2] *Department of Chemistry and Chemical Biology, University of New Mexico, Albuquerque, New Mexico, 87131, USA*

*Corresponding authors. Emails: slin@fzu.edu.cn (S.L) and hguo@unm.edu.cn (H.G.)

Abstract

The initial impulsive diffusion of hot hydrogen atoms resulted from the dissociative chemisorption of H_2 at atomically dispersed Pt atoms embedded on Cu(111) is investigated using ab initio molecular dynamics. Upon dissociation, one of the two hydrogen atoms tends to roam away from the dissociation site while the other remains trapped. It is shown that the fraction of diffusion and the average diffusion length increase with the incident energy and H_2 vibrational excitation, due apparently to the increased initial kinetic energy of the hot atoms. Most importantly, the strong interaction with surface electron-hope pairs, modeled using an electronic friction model, is shown to play an important role in rapid energy dissipation and significant retardation of the impulsive diffusion.

TOC graphic

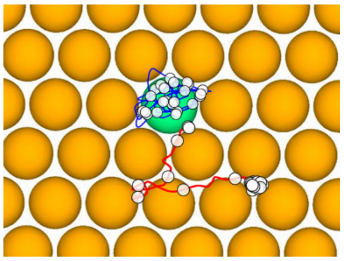

Hydrogen spillover refers to the migration of activated H atoms from hydrogen-rich regions of a catalytic surface, typically a metal, to hydrogen-poor regions, such as oxides.[1, 2] In the initial discovery,[3] atomic hydrogen resulted from the dissociative chemisorption of H_2 on Pt was found to migrate to WO_3, leading to its reduction to WO_{3-x} manifested by a color change. Since then, hydrogen spillover has attracted much attention, because it represents an important element in designing advanced catalysts with enhanced catalytic activity, selectivity, and stability.[4-6] However, the dynamics of the spillover has seldom been investigated and little is known about the factors that controls the diffusion of these activated H atoms on catalyst surfaces.

Taking advantage of hydrogen spillover, Sykes and coworkers recently created single atom alloys (SAAs) by doping copper with atomically dispersed platinum group metals (PGMs, *e.g.*, Pd and Pt),[7-13] which are found to catalyze selective hydrogenation of alkenes.[14, 15] It is well established that Cu surfaces exhibit high catalytic selectivity towards alkene hydrogenation,[16, 17] but H_2 dissociation on pure Cu has a high activation barrier and occurs very slowly unless driven by harsh reaction conditions such as high temperatures and pressures.[18] Single atoms of a PGM alloyed into Cu surfaces can significantly improve the activity of the catalyst yet retaining its high reaction selectivity in hydrogenation reactions. It was proposed that the atomically dispersed PGM active sites in the Cu-based SAA catalysts facilitate H-H bond activation, allowing for the uptake of H_2 onto the surface and promoting the subsequent H spillover onto the Cu host, where selective hydrogenation can take place.[5]

Although hydrogen spillover has previously been investigated on bimetallic

alloys,[19-21] detailed studies of hydrogen dissociation and diffusion on SAA surfaces have recently been carried out by Sykes and coworkers.[8-13] Using scanning tunneling microscopy (STM) and density functional theory (DFT), these authors found that the PGM dopants exist in atomic forms on the topmost host metal surface near step edges, thanks to their thermodynamic stability. The isolated Pd atoms on a Cu host surface were found to substantially lower the energy barrier for H_2 dissociation relative to that on Cu(111) and enable the H spillover from Pd to Cu.[8-10] Similar effects were found for atomically dispersed Pt on Cu surfaces.[13] The PGM single atoms serve as the gateway for both dissociative chemisorption and the reverse recombinative desorption of hydrogen,[11, 15] coined by Marcinkowski et al. as the "molecular cork effect".[11] Importantly, atomic H was found in regions on Cu surfaces more than hundreds of nm away from the active sites even at low temperatures.[10]

Additional studies by other groups shed further light onto the catalytic effects of PGM single atoms embedded on SAA surfaces. For example, Jiang et al. recently investigated SAA catalysts by dispersing Pd atoms onto Cu nanoparticles with different exposed facets, Cu(111) and Cu(100).[22] They revealed that Pd/Cu(100) exhibited a substantially higher catalytic activity and selectivity for the semi-hydrogenation of alkynes compared with Pd/Cu(111). By physically mixing pure copper nanomaterials with different sizes to Pd/Cu(111), they speculated that the distance of hydrogen spillover could be as long as 500 nm at room temperature. The lowering of the H_2 dissociation barrier by the PGM dopants on various Cu surfaces was also confirmed by others using DFT calculations.[23-27] Most relevant to the current work, Busnengo and

coworkers performed a DFT based ab initio molecular dynamics (AIMD) study for H_2 interacting with a Pd dopped Cu(111) surface.[23] They found that upon the dissociation at the Pd site, one H atom tends to stay near the Pd site while the other H spillovers to a nearby Cu site. In addition, H spillover from Pt and Pd clusters to their graphene substrate was investigated using AIMD,[28, 29] but the results suggested that the barriers are too high.

On metal surfaces, adsorbate diffusion and reactions are always subjected to energy dissipation via interactions with electron-hole pairs (EHPs) and lattice vibrations, i.e., phonons.[30-32] The energy dissipation strongly influences the diffuse length and relaxation time of hot atoms on the surface.[33-37] In a recent study, for example, translationally hot H atoms scattered from a gold surface were shown to loss significant energy,[38] due apparently to nonadiabatic energy dissipation to surface EHPs,[39] as the adiabatic energy transfer is minimum because of the mass disparity. EHPs are thus expected to have a significant impact on hydrogen spillover. However, all recent theoretical studies of H_2 dissociation and H diffusion on SAA surfaces[23-25] have ignored the EHPs. In this Letter, we report a first-principles study of H_2 dissociation and the initial impulsive spillover dynamics of the resulting hot H atoms on a Pt/Cu(111) SAA surface driven by their kinetic energy acquired during dissociation. Both the mechanical (adiabatic) and electronic (nonadiabatic) dissipations are treated based on AIMD, augmented by an electronic friction model (AIMDEF) in the latter case. Our results suggest that the EHP-facilitated dissipation significantly reduces the diffusion length in the initial stage of the spillover, which might have important implications in

understanding this important surface process.

All spin-polarized DFT calculations were performed in the Vienna Ab initio Simulation Package (VASP)[40, 41] using a plane wave basis with a cutoff energy of 400 eV and the projector augmented wave scheme.[42] The electron exchange-correlation was described by the optPBE-vdW functional,[43] which incorporates the van der Waals effect. The Cu(111) slab consists of four atomic layers with a 5 × 5 unit cell and separated by a vacuum space of 16 Å. The Pt/Cu(111) surface was modeled by replacing one surface Cu atom with a Pt atom, corresponding to 1/25 of the surface sites. For all the calculations performed, Cu atoms located at the bottom two layers were fixed and the remaining atoms were fully relaxed. The surface Brillouin zone was described with a Γ-point electronic wave-vector grid. The energy barriers were determined using the climbing image nudged elastic band (CI-NEB) method from the VTST tools,[44] with the force convergence criterion of 0.03 eV/Å.

The static reaction pathway of H_2 dissociation and H diffusion on the Pt/Cu(111) surface computed by DFT is depicted in Fig. 1. There is a shallow (-0.06 eV) physisorption well atop the Pt atom with the H_2 parallel to the surface 3.41 Å above the surface plane. The H-H distance (0.746 Å) is close to that of the isolated H_2 (0.751 Å). The dissociative transition state, which resembles the physisorption configuration, but is closer to the surface (Z=2.13 Å) with an H-H distance significantly elongated to 0.784 Å, is merely 0.05 eV above from the asymptote. This is consistent with the experimentally observed facile H_2 dissociation on the Pt/Cu(111) SAA surface,[15] and in agreement with previous DFT studies of this system.[15, 24, 26] The nearly barrierless

dissociation pathway is similar to that on the Pt(111),[45] in sharp contrast with that on Cu(111), which is around 0.5 eV.[18, 46, 47] After the barrier, the two H atoms settle in two adjacent hollow sites with a distance between them of 2.76 Å with a total adsorption energy of -0.34 eV, relative to the gaseous H_2. In Supporting Information (SI), a detailed comparison of the dissociation barriers on different surfaces is given.

The calculated diffusion energy barrier of a H atom from the Pt-Cu-Cu hollow site, as shown in Fig. 1, to an adjacent Cu-Cu-Cu hollow site is 0.25 eV, in agreement with previous calculations (~0.3 eV).[24, 27] The barrier for the subsequent H diffusion to a farther Cu-Cu-Cu hollow site is 0.06 eV. The diffusion of the second H away from the initial Pt-Cu-Cu site is difficult, with a barrier of 0.26 eV. As a result, the initial Pt-Cu-Cu site could serve as a trap for atomic hydrogen. As shown by the figure, energies of all diffusion barriers are below to that of the H_2(g) + Pt/Cu(111) asymptote, which make the diffusion possible. The energetics of the diffusion pathway is similar to that of the Pd/Cu(111) system as well.[8, 23]

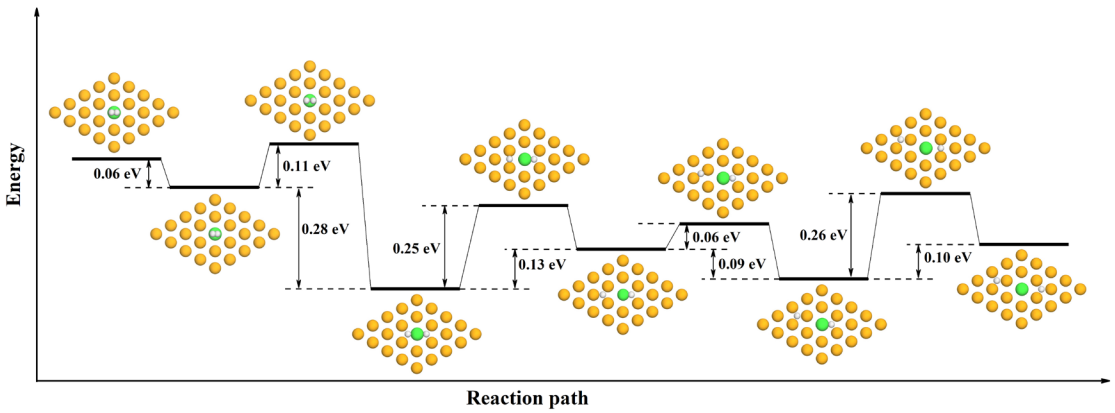

Fig. 1. Energy profile for H_2 dissociation and H diffusion on the Pt/Cu(111) surface. White, orange, and green spheres represent H, Cu, and Pt atoms, respectively. For

clarity, only the top layer of the Pt/Cu(111) surface is shown.

The AIMD and AIMDEF calculations were performed using a modified VASP program.[33-35, 48] The electronic friction was approximated with a generalized Langevin equation[49] with friction coefficients from the independent atom approximation (IAA) version[50] of the local density friction approximation (LDFA).[51, 52] The Pt/Cu(111) surface was modeled with a 5×5 unit cell, which is larger than that used in the static calculations, to explore both the adiabatic and nonadiabatic dynamics of H_2 dissociation and the subsequent hot H atom diffusion. The Brillouin zone sampling was carried out with a Γ-point electronic wave-vector grid. The metal substrate was equilibrated at 300 K for 3 ps and the geometries and momenta of surface atoms were saved for the AIMD/AIMDEF dynamic calculations. The initial position of the impinging H_2 was placed 6.0 Å above the Pt/Cu(111) surface with its polar and azimuthal rotational angles randomly sampled. The incident kinetic energy of the H_2 molecule ranges from 0.1 to 0.5 eV with the center of mass velocity along the surface normal (θ_i=0°) and at an oblique angle (θ_i=20°). The H-H internuclear distance and vibrational momentum were sampled for both the ground (v=0) and first excited state (v=1) using a quasi-classical trajectory model.[53] The time step of the AIMD calculations was set at 1.0 and 0.5 fs for the v=0 and 1 states of H_2, respectively, while the time step of AIMDEF calculations was set at 0.25 fs.

To understand the influence of the Pt dopant in H_2 dissociation and the subsequent diffusion of atomic hydrogen, we first performed the AIMD calculations with H_2(v=0,1) impinging on the Pt/Cu(111) surface at normal incidence with incident energies, E_i =

0.10, 0.25 and 0.50 eV. For each E_i value, we propagate 50 trajectories. The impinging H_2 is within a circle centered at the Pt site with a radius of r=1.4 Å, since the reactivity drops to zero outside the circle as discussed in SI. A trajectory was considered as: (I) "dissociation", if the H-H distance reached 2.3 Å; (II) "scattering", if the H_2 is scattered beyond 6.0 Å above the surface with the molecular center velocity pointing away from the surface; (III) "diffusion", if the distance between an H atom and the Pt site reached beyond 2.5 Å after H_2 dissociation; and (IV) "trapping", if the distance between an H atom and the Pt site was less than 2.5 Å after H_2 dissociation when the maximum propagation time was reached. The results are summarized in Table 1. Note that the latter two cases are necessarily contained in I: each dissociation always results in either one diffusion (III) and one trapping (IV) or two diffusion (III) events. Mathematically, the sum of the III and IV fractions should be twice of that for I. An exemplary trajectory depicting diffusion and trapping is shown in Fig. 2 and more are displayed in SI.

Table 1. Fractions of H_2 dissociation (f_{diss}), the corresponding standard errors (σ_{diss}) of H_2 dissociation, H trapping (f_{trap}), the standard errors (σ_{trap}) of H trapping, H diffusion (f_{diff}), the standard errors (σ_{diff}) of H diffusion, the mean distance of H diffusion (d_{diff}) and the maximum distance of H diffusion (D_{diff}), obtained from AIMD calculations with different initial states (IS) of H_2 and incident energies (E_i) at normal incidence.

E_i (eV)	IS	f_{diss}	f_{trap}	f_{diff}	d_{diff} (Å)	D_{diff} (Å)
0.10	v=0,j=0	10±4.2 %	12±4.6 %	8±3.8 %	9.35	10.13
0.25	v=0,j=0	16±5.2 %	18±5.4 %	14±4.9 %	9.87	16.25

0.50	v=0,j=0	46±7.0 %	38±6.9 %	54±7.1 %	10.92	21.86
0.25	v=1,j=0	34±6.7 %	22±5.9 %	46±7.1 %	12.31	22.35

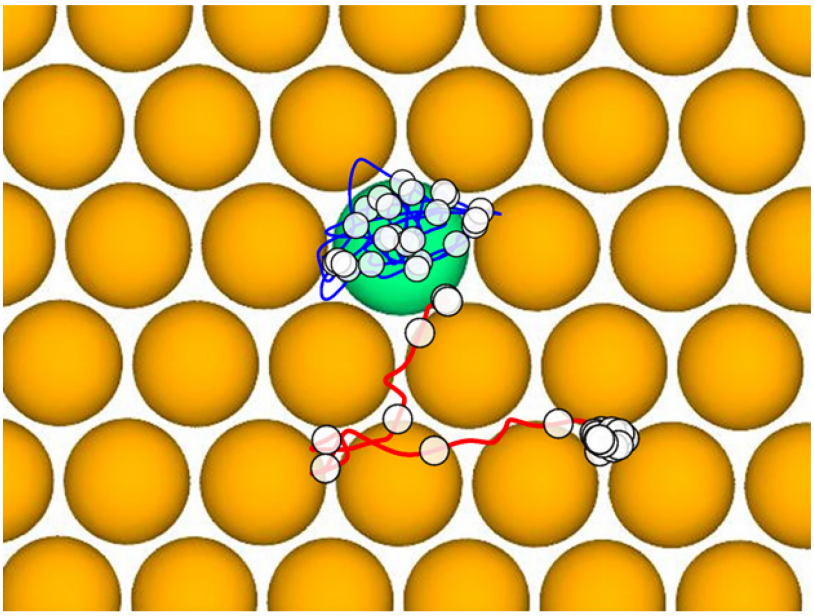

Fig. 2. An exemplary trajectory depicting diffusion and trapping of the hot H atoms upon dissociation. The blue and red lines represent trapping and diffusion trajectories, respectively. The H, Cu, and Pt atoms are represented by white, orange and green spheres, respectively. For clarity, only the top view of the atomic structures is shown.

As shown in Table 1, the fraction of dissociation increases from 10 to 46 % as the incident energy is increased from 0.1 to 0.5 eV. Despite the low barrier in Fig. 1 for H_2 dissociation at the Pt site, the corresponding potential energy surface is quite anisotropic, similar to the case on Pt(111).[45] Dissociation is most likely to occur when the H_2 molecule orients parallel to the surface and the barrier increases drastically with the polar angle of the molecule. As a result, not all trajectories lead to dissociation, as shown in Table 1, even when the energy is higher than the minimal barrier. The

dissociation is also promoted by vibrational excitation of the incident H_2, thanks to the late barrier of this process. The promotional effect of both the translational and vibrational excitation is well established by previous studies.[54]

After dissociation, the H atoms acquire on average an amount of energy equal to ($E_i + E_{\mathrm{vib}} + E_{ad}$), which renders them translationally hot and undergo extensive diffusion on the surface, as shown in Fig. 2. In most of these trajectories, one H is trapped near the Pt site while the other roams around the surface, consistent with the higher diffusion barrier for the second H atom shown in Figure 1. This is also in agreement with the recent work of Ramos et al. on H_2 dissociation and H diffusion on Pd/Cu(111).[23] At the lowest incident energy (0.10 eV), only 8% undergo diffusion, with a mean diffusion length of ~ 9 Å. As the incident energy is increased to 0.50 eV, and the fraction of H diffusion increases to 54 %, and the mean diffusion length to ~11 Å. Similarly, the vibrational excitation of the impinging H_2 also leads to increased diffusion fraction and mean/maximum diffusion length. These increases can be readily understood as the total energy available to the hot H atoms is increased. In the meantime, the trapping fraction decreases as the energy increases, either from translational or vibrational excitation.

The results presented above are all obtained from the AIMD simulations, which only included the dissipation due to surface phonons. In order to explore the impact of energy dissipation caused by surface EHPs on H diffusion, we performed AIMDEF simulations for H_2 impinging the surface at normal and oblique incidences with the incident energy of 0.25 eV. 100 trajectories are run for each case. The results are compiled in Table 2 in a similar fashion as Table 1.

Table 2. Fractions of H_2 dissociation (f_{diss}), the corresponding standard errors (σ_{diss}) of H_2 dissociation, H trapping (f_{trap}), the standard errors (σ_{trap}) of H trapping, H diffusion (f_{diff}), the standard errors (σ_{diff}) of H diffusion, the mean distance of H diffusion (d_{diff}) and the maximum distance of H diffusion (D_{spill}), obtained from AIMD and AIMDEF calculations with H_2(v=0) impinging on the Pt/Cu(111) surface at the incident energy of 0.25 eV at two different incidence angles (θ_i).

Method	θ_i(°)	f_{diss}	f_{trap}	f_{diff}	d_{diff} (Å)	D_{diff} (Å)
AIMD	0	22±4.1 %	25±4.3 %	19±3.9 %	9.84	20.53
AIMDEF	0	20±4.0 %	35±4.8 %	5±2.2 %	4.73	5.78
AIMD	20	14±3.5 %	22±4.1 %	6±2.4 %	9.60	16.32
AIMDEF	20	13±3.4 %	22±4.1 %	4±2.0 %	4.88	6.03

As shown in Table 2, it is clear that the oblique incidence reduces the dissociation fraction because the kinetic energy along the surface normal is smaller (normal scaling). Accordingly, the diffusion fraction is also lowered, although the diffusion length remains roughly the same. This result suggests oblique incidence may not help the spillover. Furthermore, the fraction of dissociation is similar for AIMD and AIMDEF calculations, indicating that EHPs have only a very limited effect on dissociation. This is consistent with existing knowledge of dissociative chemisorption.[50, 55] However, the fraction of H diffusion is drastically reduced, along with a reduced mean and maximum diffusion lengths. In other words, coupling to surface EHPs leads to strong dissipation.

Along with phonon-induced dissipation, the diffusion is significantly curtailed.

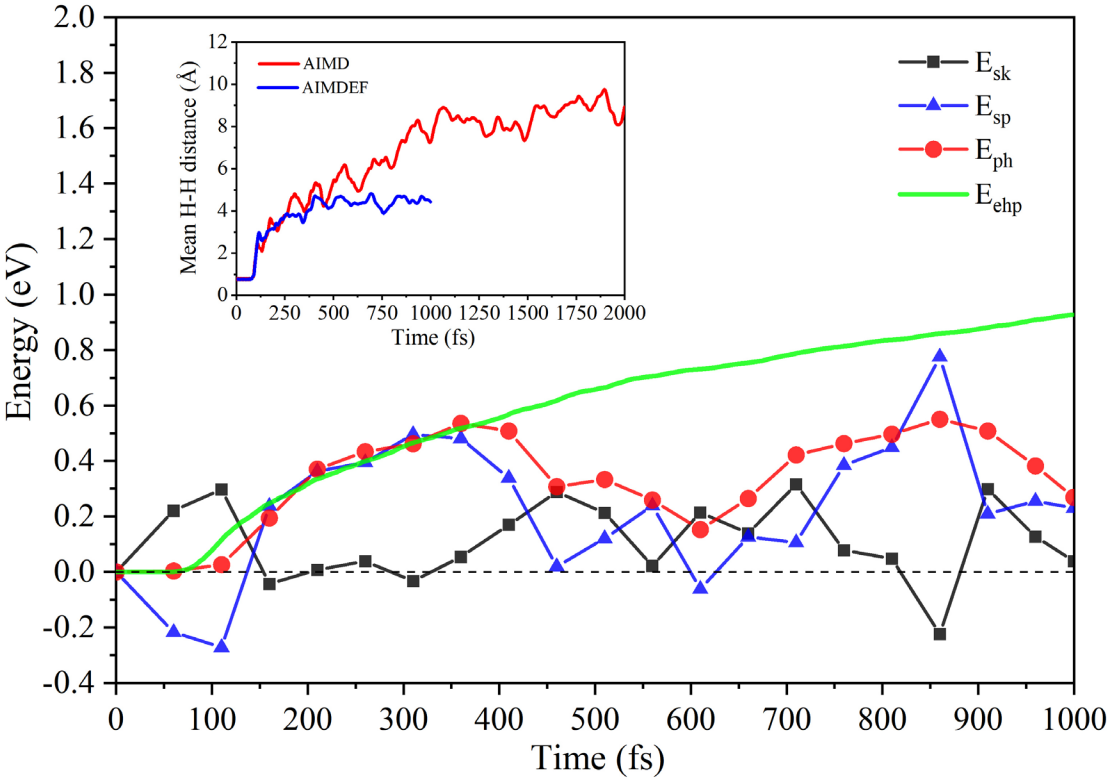

Fig. 3. Main panel: The mean energy dissipation caused by phonons ($E_{ph} = E_{sk} + E_{sp}$) and EHPs (E_{ehp}) as a function of time for the diffusion AIMDEF trajectories. Inset: the mean H-H distance of the diffusing H atoms as a function of time from the diffusion AIMD and AIMDEF trajectories.

To provide a statistical perspective of the difference between the AIMD and AIMDEF trajectories, we have computed the mean H-H distance by averaging over all diffusion trajectories for normal incidence $H_2(v=0)$ at 0.25 eV incident energy. As shown in Figure 3, the diffusion is mostly complete in 0.5 ps for AIMDEF and this time is about 1.5 ps for AIMD. The mean H-H separation is also much smaller in AIMDEF simulations than that in the AIMD ones. This result suggests that the EHPs plays a

significant role in energy dissipation and retardation of diffusion. It is worth noting that our AIMDEF calculated distance of H diffusion on the Pt/Cu(111) surface (~5 Å) is similar to the results of AIMDEF calculations for H travelling on Pd(100) (~5 Å) with the incident energies of 0.5 eV and 1.0 eV, as reported in Ref. [33].

To further quantify the effects of EHPs and phonons on the energy dissipation, we compute the energy dissipation along the trajectories. For a single trajectory, the energy dissipation caused by EHPs ($E_{ehp}(t)$) as a function of time can be evaluated by integrating the friction force on gas atom A,[35, 50]

$$E_{ehp}(t) = \int_0^t \eta\left(r_A(t')\right)|v_A(t')|^2 dt' \quad (1)$$

where $\eta(r_A)$ is the friction coefficient acting on the hydrogen atom at its position r_A, and v_A is the instantaneous atomic velocity. On the other hand, the energy dissipation caused by phonons (E_{ph}) is approximated as $E_{ph} = E_{sk} + E_{sp}$, where E_{sk} is the instantaneous variation of the kinetic energy of the surface atoms and E_{sp} is the instantaneous variation of the potential energy as a result of lattice distortions.[35] E_{sk} was provided on-the-fly in the AIMDEF simulations relative to the initial kinetic energy of the surface atoms. E_{sp} can be evaluated as the difference between the potential energy of the equilibrium bare-surface configuration and the distorted surface configuration of which adsorbate was removed.

The energy loss in individual trajectories is similar so we present the averaged results. As shown in Fig. 3, the dissipated energy due to EHPs increases monotonically and smoothly with time. This is because the friction coefficient for the H atom is quite significant and mostly constant, thanks to the fact that η is correlated with the electron

density at the H positions,[56, 57] which are quite large thanks to the small size of the atom. On the other hand, the energy loss to the phonons mostly occurs during collisions between the hot H atom and the surface, resulting in non-monotonic energy loss and sometimes even energy gain. The contribution of phonons in dissipation is comparable to that of EHPs in the run time from 100 to 400 fs, in which H diffusion takes place in this period. After 0.5 ps, the energy transfer into EHPs is around two times larger than the energy transfer into phonons.

The results presented above cannot be directly compared with the spillover length of ~10^2 nm reported in recent studies.[10, 22] We note that the simulation time in this work is on the order of a few ps, which is sufficient to follow the impulsive diffusion of the hot H atoms immediately after the dissociation, but far shorter than time needed for thermal diffusion, which can certainly contribute to spillover. Furthermore, the H atom dynamics is treated in this work with classical mechanics, which ignores tunneling. The inclusion of tunneling is expected to lower the effective diffusion barrier and helping the diffusion.[10] Finally, the electronic friction is treated approximately in this work by only considering the diagonal elements of the friction tensor. Recent advances in computing the full friction tensor using first-principles methods[58, 59] could provide a more accurate treatment of the EHP-facilitated energy dissipation.

The next level of understanding of hydrogen spillover requires an accurate account of thermal diffusion at a much longer time scale. However, this will face two major challenges. First, an accurate analytical potential energy surface is needed as AIMD is too time consuming. This has recently become possible with reliable DFT models for

the interaction energy[60] and machine learning based construction of high-dimensional potential energy surfaces.[61] The second challenge is a method capable of including quantum tunneling. A possible candidate of a quantum treatment of H diffusion is ring-polymer molecular dynamics,[62] which has been attempted recently.[63] We emphasize that thermal diffusion is expected to also be affected by dissipation (and fluctuation) due to surface phonons and electron-hole pairs.

To summarize, we have investigated using first-principles methods the impulsive diffusion of H atoms immediately after their initial dissociation at the active Pt site atomically dopped on Cu(111). Our results indicate that the hot H atoms diffuse from the initial site near the Pt to nearby Cu surface sites, and the fraction of diffusion and the diffusing length depend on the available energy acquired in the dissociation. More importantly, the H atoms are subject to strong EHPs induced dissipation, which is modeled here via an electronic friction model, and they lead to a smaller fraction of diffusion and reduced diffusion length in the AIMDEF calculations relative the AIMD results. These results underscore the importance of nonadiabatic effects in surface processes, particular those involving light atoms, whose small size allows them to access the electron density of the substrate.

Acknowledgments: This research was supported by National Natural Science Foundation of China (21673040 and 21973013 to S.L), Natural Science Foundation of Fujian Province of China (2020J02025 to S.L.), "Chuying Program" for the Top Young Talents of Fujian Province to S.L., and US National Science Foundation (CHE-1951328

to H.G.). We thank Prof. Maite Alducin for sharing with us the AIMDEF code and Prof. Bin Jiang and Dr. Linsen Zhou for stimulating discussions and technical help. H.G. also thanks Prof. Charlie Sykes for discussion on the experiment.

REFERENCES

1. Prins, R. Hydrogen spillover. Facts and fiction, *Chem. Rev.* **2012,** *112*, 2714-2738.
2. Sermon, P. A.; Bond, G. C. Hydrogen spillover, *Catal. Rev.* **1974,** *8*, 211-239.
3. Khoobiar, S. Particle to particle migration of hydrogen atoms on platinum—alumina catalysts from particle to neighboring particles, *J. Phys. Chem.* **1964,** *68*, 411-412.
4. Conner, W. C.; Falconer, J. L. Spillover in heterogeneous catalysis, *Chem. Rev.* **1995,** *95*, 759-788.
5. Hannagan, R. T.; Giannakakis, G.; Flytzani-Stephanopoulos, M.; Sykes, E. C. H. Single-atom alloy catalysis, *Chem. Rev.* **2020,** *120*, 12044-12088.
6. Xiong, M.; Gao, Z.; Qin, Y. Spillover in heterogeneous catalysis: New insights and opportunities, *ACS Catal.* **2021,** *11*, 3159-3172.
7. Tierney, H. L.; Baber, A. E.; Sykes, E. C. H. Atomic-scale imaging and electronic structure determination of catalytic sites on Pd/Cu near surface alloys, *J. Phys. Chem. C* **2009,** *113*, 7246-7250.
8. Tierney, H. L.; Baber, A. E.; Kitchin, J. R.; Sykes, E. C. H. Hydrogen dissociation and spillover on individual isolated palladium atoms, *Phys. Rev. Lett.* **2009,** *103*, 246102.
9. Baber, A. E.; Tierney, H. L.; Lawton, T. J.; Sykes, E. C. H. An atomic-scale view of palladium alloys and their ability to dissociate molecular hydrogen, *ChemCatChem* **2011,** *3*, 607-614.
10. Jewell, A. D.; Peng, G.; Mattera, M. F. G.; Lewis, E. A.; Murphy, C. J.; Kyriakou, G.; Mavrikakis, M.; Sykes, E. C. H. Quantum tunneling enabled self-assembly of hydrogen atoms on Cu(111), *ACS Nano* **2012,** *6*, 10115-10121.
11. Marcinkowski, M. D.; Jewell, A. D.; Stamatakis, M.; Boucher, M. B.; Lewis, E. A.; Murphy, C. J.; Kyriakou, G.; Sykes, E. C. H. Controlling a spillover pathway with the molecular cork effect, *Nat. Mat.* **2013,** *12*, 523-528.
12. Kyriakou, G.; Davidson, E. R. M.; Peng, G.; Roling, L. T.; Singh, S.; Boucher, M. B.; Marcinkowski, M. D.; Mavrikakis, M.; Michaelides, A.; Sykes, E. C. H. Significant quantum effects in hydrogen activation, *ACS Nano* **2014,** *8*, 4827-4835.
13. Lucci, F. R.; Marcinkowski, M. D.; Lawton, T. J.; Sykes, E. C. H. H_2 activation and spillover on catalytically relevant Pt–Cu single atom alloys, *J. Phys. Chem. C* **2015,** *119*, 24351-24357.
14. Kyriakou, G.; Boucher, M. B.; Jewell, A. D.; Lewis, E. A.; Lawton, T. J.; Baber, A. E.; Tierney, H. L.; Flytzani-Stephanopoulos, M.; Sykes, E. C. H. Isolated metal atom

geometries as a strategy for delective heterogeneous hydrogenations, *Science* **2012,** *335*, 1209.
15. Lucci, F. R.; Liu, J.; Marcinkowski, M. D.; Yang, M.; Allard, L. F.; Flytzani-Stephanopoulos, M.; Sykes, E. C. Selective hydrogenation of 1,3-butadiene on platinum-copper alloys at the single-atom limit, *Nat. Commun.* **2015,** *6*, 8550.
16. Zhao, B.; Zhang, R.; Huang, Z.; Wang, B. Effect of the size of Cu clusters on selectivity and activity of acetylene selective hydrogenation, *Appl. Catal. A* **2017,** *546*, 111-121.
17. Yang, B.; Burch, R.; Hardacre, C.; Hu, P.; Hughes, P. Selective hydrogenation of acetylene over Cu(211), Ag(211) and Au(211): Horiuti–Polanyi mechanism vs. non-Horiuti–Polanyi mechanism, *Catal. Sci. Tech.* **2017,** *7*, 1508-1514.
18. Kammler, T.; Küppers, J. Interaction of H atoms with Cu(111) surfaces: Adsorption, absorption, and abstraction, *J. Chem. Phys.* **1999,** *111*, 8115-8123.
19. Goodman, D. W.; Yates, J. T.; Peden, C. H. F. The reaction of atomic copper with chemisorbed hydrogen on ruthenium, *Surf. Sci.* **1985,** *164*, 417-424.
20. Yates, J. T.; Peden, C. H. F.; Goodman, D. W. Copper site blocking of hydrogen chemisorption on ruthenium, *J. Catal.* **1985,** *94*, 576-580.
21. Yao, Y.; Goodman, D. W. Direct evidence of hydrogen spillover from Ni to Cu on Ni–Cu bimetallic catalysts, *J. Mol. Catal. A* **2014,** *383-384*, 239-242.
22. Jiang, L.; Liu, K.; Hung, S.-F.; Zhou, L.; Qin, R.; Zhang, Q.; Liu, P.; Gu, L.; Chen, H. M.; Fu, G., et al. Facet engineering accelerates spillover hydrogenation on highly diluted metal nanocatalysts, *Nat. Nanotech.* **2020,** *15*, 848-853.
23. Ramos, M.; Martínez, A. E.; Busnengo, H. F. H_2 dissociation on individual Pd atoms deposited on Cu(111), *Phys. Chem. Chem. Phys.* **2012,** *14*, 303-310.
24. Fu, Q.; Luo, Y. Catalytic activity of single transition-metal atom doped in Cu(111) surface for heterogeneous hydrogenation, *J. Phys. Chem. C* **2013,** *117*, 14618-14624.
25. Fu, Q.; Luo, Y. Active sites of Pd-doped flat and stepped Cu(111) surfaces for H_2 dissociation in heterogeneous catalytic hydrogenation, *ACS Catal.* **2013,** *3*, 1245-1252.
26. Lv, C.-Q.; Liu, J.-H.; Guo, Y.; Wang, G.-C. Selective hydrogenation of 1,3-butadiene over single Pt1/Cu(1 1 1) model catalysts: A DFT study, *Appl. Surf. Sci.* **2019,** *466*, 946-955.
27. Zhao, G.-C.; Qiu, Y.-Q.; Liu, C.-G. A systematic theoretical study of hydrogen activation, spillover and desorption in single-atom alloys, *Appl. Catal. A* **2021,** *610*, 117948.
28. Blanco-Rey, M.; Juaristi, J. I.; Alducin, M.; López, M. J.; Alonso, J. A. Is spillover relevant for hydrogen adsorption and storage in porous carbons doped with palladium nanoparticles?, *J. Phys. Chem. C* **2016,** *120*, 17357-17364.
29. Granja-DelRío, A.; Alducin, M.; Juaristi, J. I.; López, M. J.; Alonso, J. A. Absence of spillover of hydrogen adsorbed on small palladium clusters anchored to graphene vacancies, *Appl. Surf. Sci.* **2021,** *559*, 149835.
30. Alducin, M.; Díez Muiño, R.; Juaristi, J. I. Non-adiabatic effects in elementary reaction processes at metal surfaces, *Prog. Surf. Sci.* **2017,** *92*, 317-340.
31. Rittmeyer, S. P.; Bukas, V. J.; Reuter, K. Energy dissipation at metal surfaces, *Adv. Phys. X* **2018,** *3*, 1381574.

32. Jiang, B.; Guo, H. Dynamics in reactions on metal surfaces: A theoretical perspective, *J. Chem. Phys.* **2019,** *150*, 180901.
33. Blanco-Rey, M.; Juaristi, J. I.; Díez Muiño, R.; Busnengo, H. F.; Kroes, G. J.; Alducin, M. Electronic friction dominates hydrogen hot-atom relaxation on Pd(100), *Phys. Rev. Lett.* **2014,** *112*, 103203.
34. Saalfrank, P.; Juaristi, J. I.; Alducin, M.; Blanco-Rey, M.; Díez Muiño, R. Vibrational lifetimes of hydrogen on lead films: An ab initio molecular dynamics with electronic friction (AIMDEF) study, *J. Chem. Phys.* **2014,** *141*, 234702.
35. Novko, D.; Blanco-Rey, M.; Juaristi, J. I.; Alducin, M. Ab initio molecular dynamics with simultaneous electron and phonon excitations: Application to the relaxation of hot atoms and molecules on metal surfaces, *Phys. Rev. B* **2015,** *92*, 201411(R).
36. Galparsoro, O.; Petuya, R.; Busnengo, F.; Juaristi, J. I.; Crespos, C.; Alducin, M.; Larregaray, P. Hydrogen abstraction from metal surfaces: when electron-hole pair excitations strongly affect hot-atom recombination, *Phys. Chem. Chem. Phys.* **2016,** *18*, 31378-31383.
37. Zhou, L.; Zhou, X.; Alducin, M.; Zhang, L.; Jiang, B.; Guo, H. Ab initio molecular dynamics study of the Eley-Rideal reaction of H + Cl–Au(111) → HCl + Au(111): Impact of energy dissipation to surface phonons and electron-hole pairs, *J. Chem. Phys.* **2018,** *148*, 014702.
38. Bünermann, O.; Jiang, H.; Dorenkamp, Y.; Kandratsenka, A.; Janke, S. M.; Auerbach, D. J.; Wodtke, A. M. Electron-hole pair excitation determines the mechanism of hydrogen atom adsorption, *Science* **2015,** *350*, 1346-1349.
39. Janke, S. M.; Auerbach, D. J.; Wodtke, A. M.; Kandratsenka, A. An accurate full-dimensional potential energy surface for H–Au(111): Importance of nonadiabatic electronic excitation in energy transfer and adsorption, *J. Chem. Phys.* **2015,** *143*, 124708.
40. Kresse, G.; Furthmuller, J. Efficient iterative schemes for ab initio total-energy calculations using plane wave basis set, *Phys. Rev. B* **1996,** *54*, 11169-11186.
41. Kresse, G.; Furthmuller, J. Efficiency of ab initio total energy calculations for metals and semiconductors using plane wave basis set, *Comp. Mater. Sci.* **1996,** *6*, 15-50.
42. Blöchl, P. E. Projector augmented-wave method, *Phys. Rev. B* **1994,** *50*, 17953-17979.
43. Klimeš, J.; Bowler, D. R.; Michaelides, A. Van der Waals density functionals applied to solids, *Phys. Rev. B* **2011,** *83*, 195131.
44. Henkelman, G.; Uberuaga, B. P.; Jónsson, H. A climbing image nudged elastic band method for finding saddle points and minimum energy paths, *J. Chem. Phys.* **2000,** *113*, 9901-9904.
45. Olsen, R. A.; Kroes, G. J.; Baerends, E. J. Atomic and molecular hydrogen interacting with Pt(111), *J. Chem. Phys.* **1999,** *111*, 11155-11163.
46. Hammer, B.; Nørskov, J. K. Why gold is the noblest of all the metals, *Nature* **1995,** *376*, 238-240.
47. Díaz, C.; Pijper, E.; Olsen, R. A.; Busnengo, H. F.; Auerbach, D. J.; Kroes, G.-J.

Chemically accurate simulation of a prototypical surface reaction: H_2 dissociation on Cu(111), *Science* **2009,** *326*, 832-834.
48. Novko, D.; Alducin, M.; Blanco-Rey, M.; Juaristi, J. I. Effects of electronic relaxation processes on vibrational linewidths of adsorbates on surfaces: The case of CO/Cu(100), *Phys. Rev. B* **2016,** *94*, 224306.
49. Tully, J. C. Dynamics of gas-surface interactions: 3D generalized Langevin model applied to fcc and bcc surfaces, *J. Chem. Phys.* **1980,** *73*, 1975.
50. Juaristi, J. I.; Alducin, M.; Díez Muiño, R.; Busnengo, H. F.; Salin, A. Role of electron-hole pair excitations in the dissociative adsorption of diatomic molecules on metal surfaces, *Phys. Rev. Lett.* **2008,** *100*, 116102.
51. Hellsing, B.; Persson, M. Electronic damping of atomic and molecular vibrations at metal surfaces, *Phys. Scr.* **1984,** *29*, 360-371.
52. Li, Y.; Wahnström, G. Nonadiabatic effects in hydrogen diffusion in metals, *Phys. Rev. Lett.* **1992,** *68*, 3444-3447.
53. Hase, W. L., Classical trajectory simulations: Initial conditions. In *Encyclopedia of Computational Chemistry*, Alinger, N. L., Ed. Wiley: New York, 1998; Vol. 1, pp 399-402.
54. Pijper, E.; Kroes, G. J.; Olsen, R. A.; Baerends, E. J. Reactive and diffractive scattering of H_2 from Pt(111) studied using a six-dimensional wave packet method, *J. Chem. Phys.* **2002,** *117*, 5885-5898.
55. Jiang, B.; Alducin, M.; Guo, H. Electron–hole pair effects in polyatomic dissociative chemisorption: Water on Ni(111), *J. Phys. Chem. Lett.* **2016,** *7*, 327-331.
56. Echenique, P. M.; Nieminen, R. M.; Ritchie, R. H. Density functional calculation of stopping power of an electron gas for slow ions, *Solid State Commun.* **1981,** *37*, 779-781.
57. Echenique, P. M.; Nieminen, R. M.; Ashley, J. C.; Ritchie, R. H. Nonlinear stopping power of an electron gas for slow ions, *Phys. Rev. A* **1986,** *33*, 897-904.
58. Maurer, R. J.; Jiang, B.; Guo, H.; Tully, J. C. Mode specific electronic friction in dissociative chemisorption on metal surfaces: H_2 on Ag(111), *Phys. Rev. Lett.* **2017,** *118*, 256001.
59. Spiering, P.; Meyer, J. Testing electronic friction models: Vibrational de-excitation in scattering of H_2 and D_2 from Cu(111), *J. Phys. Chem. Lett.* **2018,** *9*, 1803-1808.
60. Kroes, G.-J. Computational approaches to dissociative chemisorption on metals: towards chemical accuracy, *Phys. Chem. Chem. Phys.* **2021,** *23*, 8962-9048.
61. Jiang, B.; Li, J.; Guo, H. High-fidelity potential energy surfaces for gas phase and gas-surface scattering processes from machine learning, *J. Phys. Chem. Lett.* **2020,** *11*, 5120-5131.
62. Habershon, S.; Manolopoulos, D. E.; Markland, T. E.; Miller III, T. F. Ring-polymer molecular dynamics: Quantum effects in chemical dynamics from classical trajectories in a extended phase space, *Annu. Rev. Phys. Chem.* **2013,** *64*, 387-413.
63. Suleimanov, Y. V. Surface diffusion of hydrogen on Ni(100) from ring polymer molecular dynamics, *J. Phys. Chem. C* **2012,** *116*, 11141-11153.